

Core-shell structured electrode materials for lithium ion batteries

H. P. Zhang · L. C. Yang · L. J. Fu · Q. Cao · D. L. Sun ·
Y. P. Wu · R. Holze

Received: 9 December 2008 / Revised: 30 January 2009 / Accepted: 10 February 2009 / Published online: 6 March 2009
© Springer-Verlag 2009

Abstract Recent progress in studies of several types of core-shell structured electrode materials, including TiO_2/C , Si/C , Si/SiO_x , LiCoO_2/C , and LiFePO_4/C nanocomposites, including details of their preparation and their electrochemical performance is briefly reviewed. Results clearly show that the coating shell can effectively prevent the aggregation of the nanosized cores, which are the electrochemically active materials. In addition, the diffusion coefficients of lithium ions can be increased, and the reversibility of lithium intercalation and deintercalation is improved. As a result, the cycling behavior is greatly improved. The reviewed results suggest that core-shell nanocomposites are a good starting point for further development of new promising electrode materials.

Introduction

The development of lithium ion batteries has been rapid since the early 1990s; currently, its capacity density can be above 180 Wh/kg and the number of possible charge/discharge cycles can be above 2,000 [1]. However, with further development of electronics, electric vehicles, and other equipment, even higher performance is required.

H. P. Zhang · L. C. Yang · L. J. Fu · Q. Cao · D. L. Sun · Y. P. Wu
New Energy and Materials Laboratory (NEML),
Department of Chemistry, Fudan University,
Shanghai 200433, China

Y. P. Wu
e-mail: wuyup@fudan.edu.cn

R. Holze (✉)
Institut für Chemie, Technische Universität Chemnitz,
AG Elektrochemie, Strasse der Nationen 62,
09111 Chemnitz, Germany
e-mail: rudolf.holze@chemie.tu-chemnitz.de

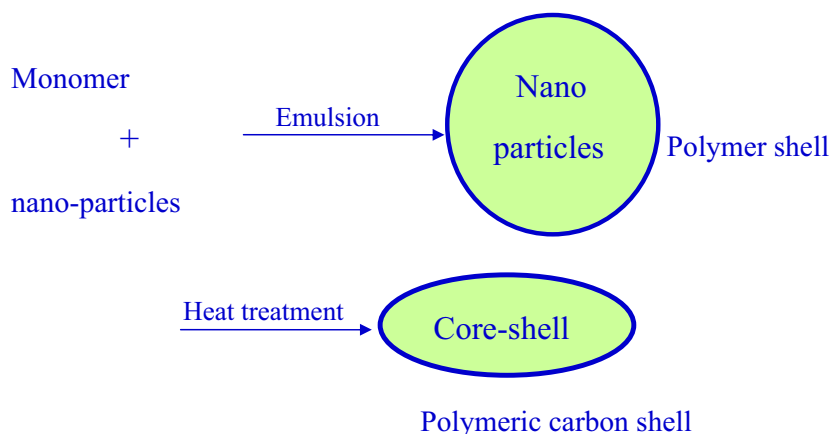
Manufacturing technology as a conceivable source of improvements has arrived at its limit. Consequently, further improvements depend on advanced electrode materials providing better performance in terms of energy and power density, rate capability, and cycle number. In this paper, we briefly review our recent progress on core-shell structured anode and cathode materials with attention to synthetic, solid-state chemistry, and electrochemical aspects [2–5].

Experimental

The preparation process for core-shell TiO_2/C is shown in Scheme 1. The details of a typical run are as follows [2]. OP_9 (1.2 g, a neutral surfactant from Guoyao Chem. Group) was dispersed in deionized water (200 ml) to form micelles. Titanium oxide nanoparticles (2.5 g, rutile structure, average diameter 15 nm, Haitai Company, China, hydrophobic surface) were added and ultrasonicated for 30 min to achieve uniform dispersion. A mixture of 2,2'-azobis(isobutyronitrile) (0.015 g, initiator) and acrylonitrile (3.0 g, monomer) was added. Degassing was carried out for 1 h under gentle stirring; then, the temperature was increased to 60°C, and the mixture was polymerized for 12 h under argon atmosphere to form a core-shell-shaped $\text{TiO}_2/\text{polyacrylonitrile}$ (PAN) precursor. After precipitating and drying, the TiO_2/PAN precursor was heat-treated at 800 °C to turn the PAN shell into a carbon shell; thus, a core-shell TiO_2/C nanocomposite was synthesized.

The preparation process of a core-shell structured Si/C nanocomposite is similar to Scheme 1. The silicon nanoparticles (spherical, $d \leq 50$ nm) were obtained from Zhongchao Company, China. After getting Si/PAN precursor by centrifugal filtration and drying, the precursor was heat-treated for 6 h at 800 °C to carbonize the PAN to get Si/C nanocomposites.

Scheme 1 Preparation process for core-shell nanocomposites based on polymeric carbon shells



A Si/SiO₂ nanocomposite was synthesized by the following process: 20 ml ethanol was mixed with 20 ml deionized water and 10 ml (0.045 mol) tetraethoxysilane. After stirring at 60 °C for 1.5 h, 1.26 g (0.045 mol) Si nanoparticles was added and ultrasonicated for 1 h to achieve a uniform sol by using ammonia solution to adjust pH to 8–9. The as-obtained mixture was then aged at 60 °C for 1 h to form a gel. The gel was further aged at room temperature for 1–2 days and dried at 70 °C for 6 h to remove volatile components, then milled to powder. The obtained powder was heated at 200 °C for 3 h and then at 500 °C for 6 h under argon atmosphere; thus, the Si/SiO₂ nanocomposite was obtained.

The carbon-coated nano-LiFePO₄ samples were prepared by a solid-state route. The starting materials Li₂CO₃, FeC₂O₄·2H₂O, NH₄H₂PO₄, and acetylene black (0, 5, 10, and 20 wt.%) were mixed at a ratio of Li/Fe/PO₄=1:1:1 in a planet mixer (QM-BP) for 24 h. The mixtures were calcified in a tube furnace at 750 °C for 15 h in an inert atmosphere.

LiCoO₂ (no. 747), a commercial product purchased from Ruixiang New Material Company (Changsha, Hunan, China), was used as starting material and reference sample. The purchased LiCoO₂ was firstly mixed with 5% sucrose (weight) in an agate mortar, then transferred to a planet mixer (QM-BP), and milled at 300 rpm for 24 h. After milling, the mixture was calcined at 600 °C for half an hour in the air.

X-ray diffraction (XRD) was performed with a Rigaku RINT-2000 diffractometer equipped with Cu/K α radiation. Scanning electron micrographs (SEM) and transmission electron micrographs (TEM) were obtained with a Philip XL30 scanning electron microscope and a JEOL JEM 2011 instrument, respectively, the elementary composition was primarily determined by energy dispersive spectroscopy.

Electrochemical performance was measured with coin-type half cells assembled as follows. The active pristine electrode materials or the core-shell nanocomposites were mixed with acetylene black as a conductive additive and

poly(vinylidene fluoride) as a binder. The mixture was coated onto a copper (for anode) or aluminum (for cathode) foil as carrier and current collector. After drying, the foils were cut into small pieces and assembled into coin-type model cells under argon atmosphere in a glove box. These pieces were used as working electrodes, lithium metal as the counter and reference electrode, Celgard 2400 as the separator, and 1 mol l⁻¹ LiPF₆ diethyl carbonate, ethylene carbonate, dimethyl carbonate (DEC/EC/DMC; w/w/w, 1:1:1 wt.%) as the electrolyte solution. Cycling tests of the half cells were performed at a constant current. Cyclic voltammograms (CV) of the electrodes were also measured. For CVs, the working electrode was small in comparison to the lithium metal electrode; thus, obtained results are dominated by the working electrode despite the use of a two-electrode arrangement. Electrochemical impedance spectra (EIS) were obtained with an EG&G M273 potentiostat/galvanostat connected to a M5210 lock-in amplifier electrochemical analysis system in the frequency range 0.1–100 kHz.

Results and discussion

Core-shell structured anode based on TiO₂

As Scheme 1 shows, this process is quite different from the reported methods to synthesize core-shell nanocomposites, which mainly include polymer coating, self-assembly, and layer-by-layer formation [6]. The principle of our process is as follows. It is known that OP₉ is a neutral surfactant with hydrophilic –O– groups and hydrophobic –CH₂–CH₂– groups; thus, stable micelles of OP₉ are formed in aqueous solution with the hydrophobic groups inside. The added nanoparticles of titanium oxide have hydrophobic surfaces and were embedded into the inner volume of the formed micelles to form a stable suspension. Monomeric acrylonitrile is also hydrophobic and entered into the inner volume of the micelles. After polymerizing at 60 °C, the monomer

was turned into a polymer. As a result, a core-shell-shaped nano-TiO₂/PAN precursor was synthesized via emulsion polymerization. Subsequently, after precipitation from water and drying, the precursor was heat-treated under argon atmosphere. It is well known that this kind of heat-treatment will turn the polymer into carbon [7]. As a result, core-shell structured TiO₂/C nanocomposites were prepared; a typical micrograph is shown in Fig. 1. It presents a well-defined core-shell structure with the core attached more closely to the carbon shell in comparison with structures synthesized via other reported ways [8].

Discharge and charge curves of pristine TiO₂ and the TiO₂/C (87:13 w/w) nanocomposite electrodes in 1 mol·l⁻¹ LiPF₆ DEC/EC/DMC (w/w/w, 1:1:1) are shown in Fig. 2. A pristine TiO₂ nanoparticle anode shows a rapid capacity fading. It is well known that nanoparticles have high surface energy and can aggregate easily; this is a common and serious problem affecting their stability. TiO₂ nanoparticles agglomerate more easily due to lithium intercalation and deintercalation. As a result, the nanoparticles gradually lost their “nano-characteristics” during cycling and showed capacity fading. In the case of the TiO₂/C nanocomposite, the charge and discharge capacity of the carbon shell in the nanocomposite can be ignored, since the intercalation voltage of lithium ion into the amorphous carbon material prepared in this study is below 0.8 V [7]. After ten cycles, the charge capacity still remains at 96.7% (i.e., 118 mAh g⁻¹ of titania) of its original capacity (i.e., 122 mAh g⁻¹ of titania), which is much higher than that of the pristine TiO₂ nanoparticles. The latter retained only 67.5% of the original capacity after ten cycles. This demonstrates that TiO₂/C core-shell nanocomposite shows a better capacity retention. The main reason is that the carbon shell suppressed the aggregation of the TiO₂ nanoparticles. In contrast, in the case of Sn/C core-shell nanocomposite, capacity still faded very

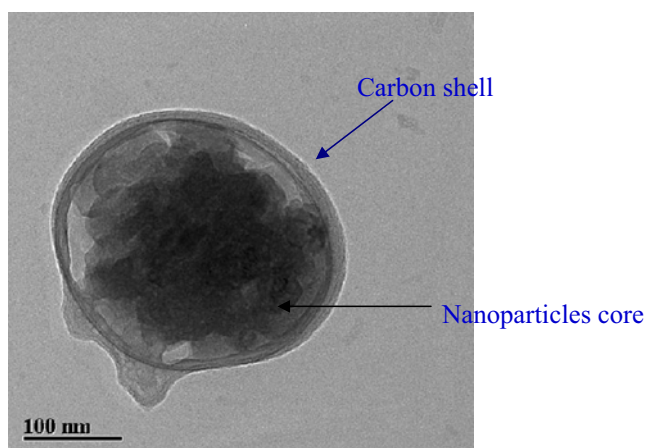


Fig. 1 Transmission electron micrograph of TiO₂/C core-shell nanocomposite

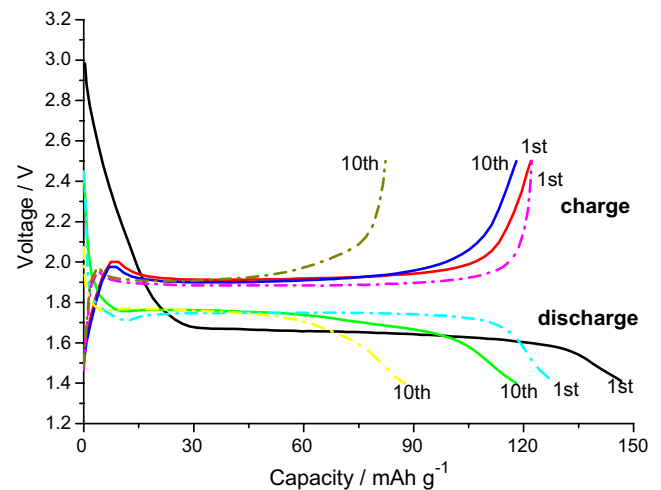


Fig. 2 Discharge and charge profiles of TiO₂ nanoparticles and TiO₂/C core-shell nanocomposite at a constant current density of 0.25 C between 1.4 and 2.5 V (solid line TiO₂/C; dashed line TiO₂)

evidently [8] since the tin core combines only loosely with the carbon shell.

The apparent diffusion coefficient measured by CV for the TiO₂/C nanocomposite (1.07×10^{-8} cm²/s) is about one order of magnitude higher than that in the virginal TiO₂ nanoparticles (1.97×10^{-9} cm²/s), indicating that the carbon shell at the surface of TiO₂ nanoparticles is beneficial for the diffusion of lithium ions, since it favors the movement of electrons; subsequently, the rate capability including the abovementioned cycling performance will be greatly improved.

Core-shell structured anode based on nanosized silicon

Since the preparation process is similar to that of TiO₂/C core-shell nanocomposite, the performance of Si/C core-shell nanocomposites will be the same. TEM show that the Si nanoparticles are linked by carbon shells uniformly and do not aggregate together. The carbon shell, about 3–5-nm thick, was successfully coated on the Si core [9].

The discharge and charge measurement shows that the Si nanoparticles have a large irreversible capacity of about 1,200 mAh g⁻¹. In contrast, the irreversible capacity of the Si/C nanocomposite is about 600 mAh g⁻¹, only half that of Si. This is mainly ascribed to the following two aspects: (1) When the surface area of the anode is larger, usually the corresponding area available for formation of the surface-electrode interface¹ (SEI) film will be larger [1]. After the nanoparticles are coated with a carbon shell, the surface area will decrease due to the smoothing effect of the shell, and the corresponding amount for SEI film will decrease.

¹ Sometimes, SEI is used for solid-electrolyte interface also.

(2) The SEI film on the carbon surface can be easily formed due to small expansion after lithium insertion. In contrast, the expansion of Si during lithium insertion results in metastable noncrystalline phases, and the accompanying formation of fresh SEI is almost always needed [10].

As mentioned above, the carbon shell is amorphous, and lithium ions can pass through the micropores. It does not affect the electrochemical performance of Si cores. However, the original reversible capacity of Si/C nanocomposite ($1,137 \text{ mAh g}^{-1}$) is lower than that of pristine Si nanoparticles ($1,831 \text{ mAh g}^{-1}$). The reversible capacity of carbon shell lower than that of Si is the main reason [1]. CVs of Si and Si/C electrodes measured between 0 and 2.0 V at a scan rate of $0.5 \text{ mV}\cdot\text{s}^{-1}$ show that the oxidation and reduction peak currents (I_p) are much higher than those of the virgin Si nanoparticles, demonstrating a better Li^+ activity of Si nanoparticles after coating with the carbon shell. The oxidation peak current at different scan rates is proportional to the root of the scan rate, $v^{1/2}$, indicating that the reaction kinetics are controlled by diffusion. Based on the linear relationship between I_p and $v^{1/2}$, the apparent diffusion coefficients of lithium ions in both Si/C nanocomposite and Si nanoparticles were calculated to be 9.68×10^{-13} and $1.09 \times 10^{-13} \text{ cm}^2 \text{ s}^{-1}$, respectively, indicating that the carbon shell on the surface of the Si nanoparticles is beneficial for the diffusion of lithium ions since it is conductive.

When comparing the cycling behavior of Si and Si/C electrodes, the former show a rapid capacity fading and retain only 6.5% of the original capacity after 20 cycles. However, in the case of the latter, after 20 cycles, the charge capacity still remains at 52.5% (594 mAh g^{-1}) of its original capacity ($1,137 \text{ mAh g}^{-1}$) much higher than that of the Si material. This shows that the Si/C core-shell nanocomposite has better capacity retention. The carbon-coating shell acting as a barrier, preventing the aggregation

of Si nanoparticles, and thus increasing their structural stability during cycling is the main reason.

After SiO was coated on the surface of Si nanoparticles, CV curves show that the separation between reduction and oxidation peaks (ΔE) of Si/SiO nanocomposite in comparison with that of the pristine Si nanoparticles is evidently smaller, indicating that the reversibility of lithium insertion and extraction of Si after coating with SiO nanoparticles is improved. Moreover, compared with the pristine Si, the ratio between the currents of reduction and oxidation peaks for the Si/SiO is much smaller, suggesting a better coulombic efficiency for the Si/SiO nanocomposite [3, 11].

The charge/discharge curves of the Si/SiO composite in the first cycle (Fig. 3a) show that the Si/SiO nanocomposite has higher coulombic efficiency (75%) in the first cycle than the virgin Si nanoparticles (70%), consistent with the results from CV. In case of the cycling behavior of the Si/SiO nanocomposite (Fig. 3b), after 20 cycles, the charge capacity still remains at 65% (538.9 mAh g^{-1}) of its original capacity (827.3 mAh g^{-1}), which is much higher than that of the pristine Si, indicating that the capacity retention of the Si/SiO nanocomposite is good. This indicates that the coated SiO, like the above carbon coating, can act as a barrier to prevent the aggregation of the Si nanoparticles, which is clearly shown by the SEM (Fig. 4) of the composite after 20 cycles.

Core-shell structured cathode based on LiFePO_4

LiFePO_4 is a cathode material considered to be an ideal substitute for LiCoO_2 because of its high capacity of 170 mAh g^{-1} , abundant resources, and environmental benignancy. The main disadvantage is its low conductivity [1, 12]; its capacity decreases rapidly with current density, which hinders its practical application. It was reported that

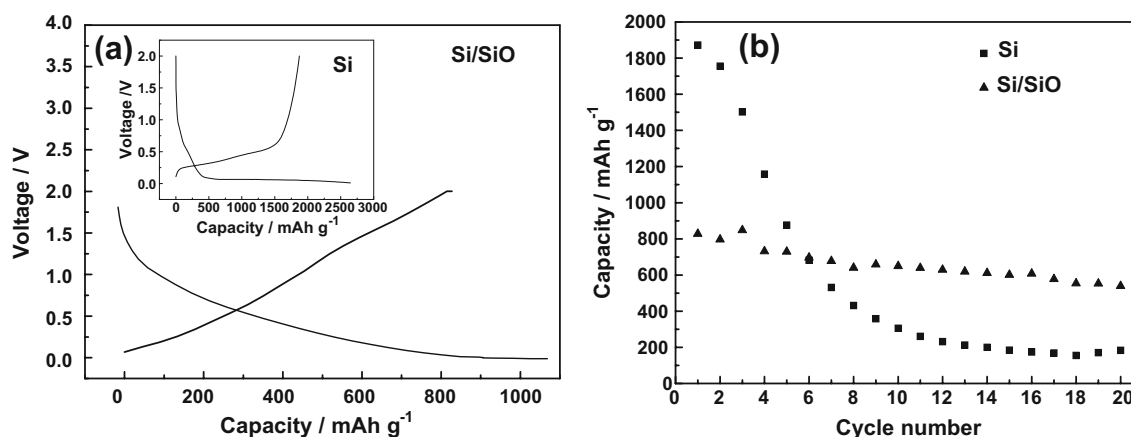
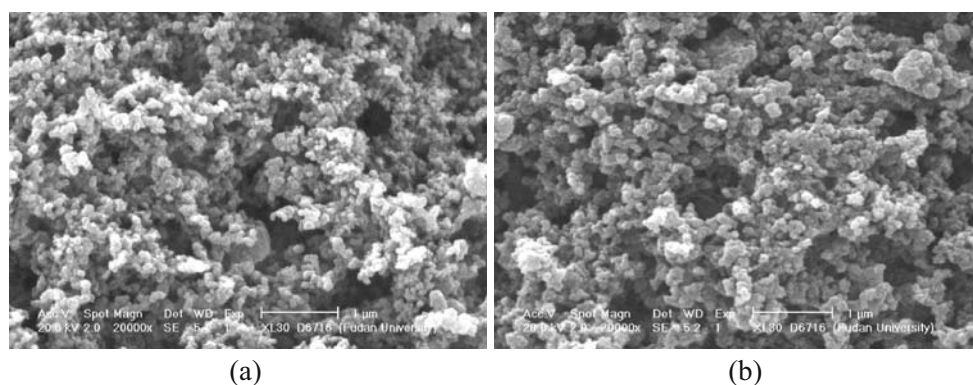


Fig. 3 Electrochemical performance of the Si/SiO core-shell composite: **a** discharge and charge curves in the first cycle and **b** the cycling behavior

Fig. 4 Morphology of the Si/SiO core-shell composite **a** before and **b** after 20 cycles



the drawbacks could be overcome by doping with multivalent elements, admixing with carbons, and preparing in the form of nanosized material [13, 14]. TEM of the carbon-coated LiFePO₄ show that the carbon completely coated the surface of LiFePO₄ particles, the composite is homogeneous, and the particles of the coated LiFePO₄ are spherical in shape with a size around 100 nm, smaller than the one obtained by solid-state reaction [15]. The unique morphology and size of the carbon-coated nanocomposites are due to the admixing of carbon in the starting material, which protected LiFePO₄ from agglomerating into larger particles. In the case of practical application, the spherical shape is preferred due to good processing performance.

CV profiles of the original and carbon-coated LiFePO₄ samples show that at the scan rate of 0.5 mV·s⁻¹, the anodic/cathodic peaks of untreated LiFePO₄ are located at 4.08/2.88 V, and *I*_p of the redox peaks is around 10⁻⁵ A [4]. The big separation between redox peaks (ΔE) of 1.20 V indicates that the electrochemical behavior is controlled by the diffusion step. In contrast, the *I*_p of the carbon-coated LiFePO₄ materials apparently increases with the content of carbon. When the content of carbon is 5, 10, and 20 wt.%, the *I*_p increases to 4.95 × 10⁻⁴, 8.69 × 10⁻⁴, and 1.32 × 10⁻³ A, respectively. Meanwhile, the ΔE between redox peaks is narrowed to 0.97, 0.70, and 0.64 V, respectively. Both *I*_p and ΔE data confirm that the kinetics of lithium intercalation and deintercalation are greatly improved by the carbon coating. This in turn will enhance the reversibility and the rate capability of the cathode composite and make its application possible.

Charge and discharge curves in the first cycle of the electrodes are shown in Fig. 5. The initial charge/discharge capacity of the pure LiFePO₄ are 106 and 22 mAh·g⁻¹; the irreversible capacity is as high as 85 mAh·g⁻¹. After coating with 5, 10, and 20 wt.% carbon, the charge/discharge capacity increases to 100/88, 158/136, and 159/128 mAh·g⁻¹, respectively. This shows clearly that the carbon coating can markedly improve the reversible capacity of LiFePO₄ nanoparticles by increasing the kinetics of lithium intercalation and deintercalation as implied by these results obtained from CV.

Following this coating process to get core-shell structured LiFePO₄/C nanocomposites, Zn²⁺ ions can be further doped into them to effectively improve the kinetics of intercalation and deintercalation of lithium ions to and from LiFePO₄, since Zn²⁺ ions do not destroy the lattice structure and enlarge the lattice volume. During deintercalation and intercalation of lithium ions, the dopant zinc atoms protect the LiFePO₄ crystal from shrinking. This kind of “pillar” effect provides larger space for the movement of lithium ions. Consequently, the conductivity is enhanced, and the lithium ion diffusion coefficient is boosted after doping. These favorable changes are beneficial to the improvement of the electrochemical performance of LiFePO₄, including discharge capacity and rate capability [16]. Besides, other heteroatoms such as Ti, Zr, V, Nb, and W can also be doped into the LiFePO₄ lattice [17, 18]. Though it was said that the electronic conductivity was increased markedly, there are some doubts on this result since carbon was introduced. We found that with a small amount (1 mol%) of dopant, the lattice structure of LiFePO₄ was not destroyed, and the reversibility of lithium ion intercalation and deintercalation was improved. The diffusion coefficient of lithium ions

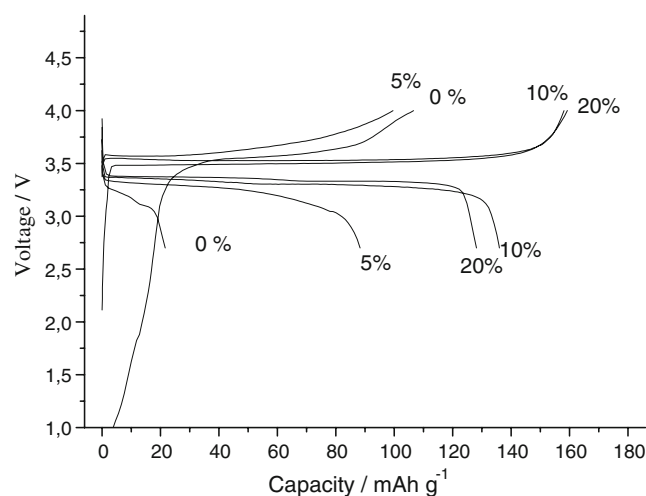


Fig. 5 The charge/discharge profiles in the first cycle of the LiFePO₄ samples at a constant current density of 0.2 mA·cm⁻² (C/10) at the voltage range of 2.5–4.0 V

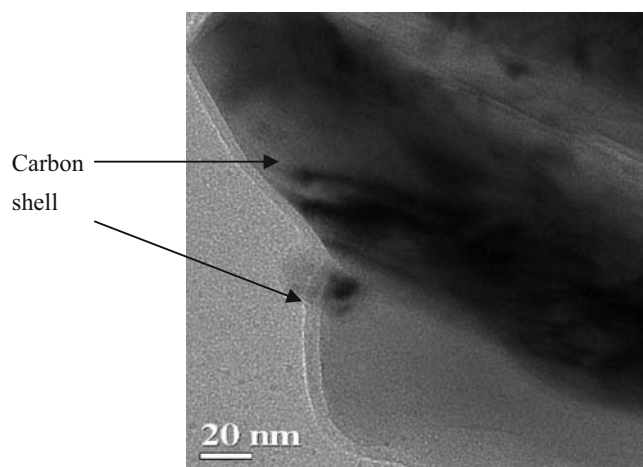


Fig. 6 TEM micrograph of the core-shell structured LiCoO_2/C

depends on the radius of the heteroatoms. When the radius of the heteroatom is larger, the coefficient increases since the lattice is enlarged [18].

The discussed processes are based on mechanical milling to coat carbon on the surface of LiFePO_4 . If the precursor is not carbon but another organic or polymeric materials such as sugar, it is also possible to obtain carbon-coated LiFePO_4 nanocomposite, and there is not much difference between their electrochemical performances [19].

Core-shell structured cathode based on LiCoO_2

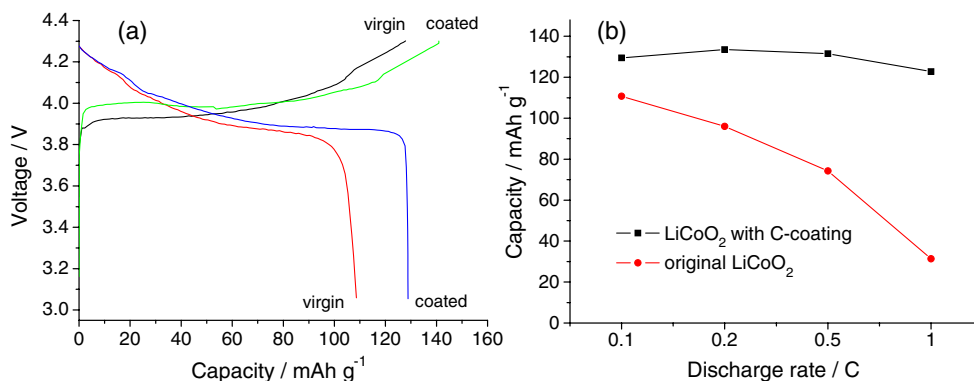
Transmission electronic micrograph of the core-shell structured LiCoO_2/C is shown in Fig. 6. A nanometer-thick carbon shell on LiCoO_2 is clearly identified [4]. Evidently, a nanolayer carbon shell was formed during the heat-treatment process. After milling in the planet mixer for a long time, the sucrose was well mixed with the LiCoO_2 . With further calcination, the sucrose decomposed into conductive carbon and was coated onto the surface of LiCoO_2 particles. Of course, the calcination time is an

important factor. Too long or too short is not a good choice. XRD patterns show that the original LiCoO_2 and the core-shell structured LiCoO_2/C have well-defined rhombohedral structure; there is only a slight decrease in the intensity of the peaks for the core-shell composite. This indicates that the amount of the coated carbon is very small. Since the calcination temperature is below $1,000^\circ\text{C}$, it is proposed that the coated carbon is amorphous [1]. Though LiCoO_2 is prone to be reduced by carbon during the heat-treatment, however, no peaks of CoO or Co_3O_4 are observed. This indicates that this carbon-coating process does not destroy the structure of LiCoO_2 or reduce LiCoO_2 . It is well known that a good rhombohedral structure can ensure good cycling of LiCoO_2 as cathode material for lithium ion battery, so the cycling behavior of the carbon-coated LiCoO_2 will be good.

Typical Nyquist plots of the core-shell structured and the original LiCoO_2 electrodes show that the charge transfer resistance R_{ct} of the former material is markedly decreased compared with the latter one. The calculated diffusion coefficients of lithium ions in the original and the carbon-coated LiCoO_2 are 1.21×10^{-10} and $1.73 \times 10^{-8} \text{ cm}^2 \text{ s}^{-1}$, respectively. Obviously the diffusion coefficient of lithium ion is greatly increased by carbon shell, suggesting that the carbon shell contributes to the enhancement of conductivity [4], which will be favorable for the electrochemical performance during cycling at high rate.

The first charge–discharge curves of the original and the core-shell structured LiCoO_2/C at 0.1 C and the relationship between the capacity and the discharge rate are shown in Fig. 7. Both of them show typical characteristics of LiCoO_2 . After coating, the charge capacity increases from 128 to 141 mAh g^{-1} , and the discharge capacity increases from about 110 to 130 mAh g^{-1} . The discharge capacity of pristine LiCoO_2 is usually about 140 mAh g^{-1} , higher than our results. The main reason is due to the different thickness of the electrode. In our case, the thickness is about $300 \mu\text{m}$, much higher than the usual one ($<100 \mu\text{m}$). The carbon-coated LiCoO_2 shows nearly no deterioration at

Fig. 7 **a** Charge and discharge curves at a rate of 0.1 C in the first cycle and **b** discharge capacity at different discharge rates of the original and the carbon-coated LiCoO_2



the rates of 0.1 to 1 C. Even at 1 C the capacity can reach 123 mAh g⁻¹, whereas the capacity of the original material degenerates greatly and the capacity remains at only 31.4 mAh g⁻¹ at 1 C. The results illustrate that the carbon shell results in superior rate capability compared with the original one, which is in accordance with the EIS results and consistent with the results on other carbon shell materials with cores of TiO₂, LiFePO₄, and Si [2, 4].

Conclusions

The various nanomaterials reviewed above show good rate capability and high reversible capacity due to their short distance for diffusion of lithium ions. However, the nanoparticles will aggregate very easily, and the nanocharacteristics will disappear. After coating a nanolayer of, e.g., carbon or SiO_x (0 < x < 2), core-shell structured nanocomposites were formed. The coatings prevent the aggregation of nanoparticles of, e.g., TiO₂ and Si, which are used as active anode materials. As a result, their cycling behavior is greatly improved. In addition, the reversibility of intercalation and deintercalation of lithium ions and diffusion of lithium ions are also better.

The carbon shell on cathodes such as LiFePO₄ and LiCoO₂ can also greatly improve their rate capability and reversible capacity due to the increase of electronic conductivity and diffusion coefficient of lithium ions.

Of course, a shell of carbon and other materials can also improve the performance of other electrode materials such as spinel Li₄Ti₅O₁₂ and LiCo_{1/3}Ni_{1/3}Mn_{1/3}O₂ [20–22], which will be a promising direction for future development of electrode materials for lithium ion batteries extending well beyond this review.

Acknowledgment Financial support from National Basic Research Program of China (973 program no. 2007CB209702), Natural Science Foundation Committee of China (50573012) and Alexander von Humboldt Foundation (Institutional Academic Cooperation Program) is gratefully appreciated.

References

1. Wu YP, Zhang HP, Wu F, Li ZH (2007) Polymer lithium ion batteries. Chemical Industry Press, Beijing
2. Fu LJ, Liu H, Zhang HP, Li C, Zhang T, Wu YP, Holze R, Wu HQ (2006) *Electrochem Commun* 8:1 doi:10.1016/j.elecom.2005.10.006
3. Zhang T, Gao J, Zhang HP, Yang LC, Wu YP, Wu HQ (2007) *Electrochem Commun* 9:886 doi:10.1016/j.elecom.2006.11.026
4. Liu H, Li C, Zhang HP, Fu LJ, Wu YP, Wu HQ (2006) *J Power Sources* 159:717 doi:10.1016/j.jpowsour.2005.10.098
5. Cao Q, Zhang HP, Wang GJ, Xia Q, Wu YP, Wu HQ (2007) *Electrochem Commun* 9:1228 doi:10.1016/j.elecom.2007.01.017
6. Caruso F (2001) *Adv Mater* 13:11 doi:10.1002/1521-4095(200101)13:1<11::AID-ADMA11>3.0.CO;2-N
7. Wu YP, Wan CR, Fang SB, Jiang YY (1999) *Carbon* 37:1901 doi:10.1016/S0008-6223(99)00067-6
8. Lee KT, Jung YS, Oh SM (2003) *J Am Chem Soc* 125:5652 doi:10.1021/ja0345524
9. Zhang T, Fu LJ, Gao J, Yang LC, Wu YP, Wu HQ (2006) *Pure Appl Chem* 78:1889 doi:10.1351/pac200678101889
10. Limthongkul P, Jang Y, Dudney NJ, Chiang YM (2003) *J Power Sources* 119–121:604 doi:10.1016/S0378-7753(03)00303-3
11. Zhao NH, Fu LJ, Yang LC, Zhang T, Wang GJ, Deng YH, Wu YP, van Ree T (2008) *Pure Appl Chem* 80:2283 doi:10.1351/pac200880112283
12. Padhi AK, Nanjundaswamy KS, Goodenough JB (1997) *J Electrochem Soc* 144:1188 doi:10.1149/1.1837571
13. Chung SY, Bloking J, Chiang YM (2002) *Nat Mater* 1:123 doi:10.1038/nmat732
14. Dominko R, Goupil JM, Bele M, Gaberscek M, Remskar M, Hanzel D, Jamnik J (2005) *J Electrochem Soc* 152:A858 doi:10.1149/1.1872674
15. Zane D, Carewska M, Scaccia S, Cardellini F, Prosini PP (2004) *Electrochim Acta* 49:4259 doi:10.1016/j.electacta.2004.04.022
16. Liu H, Cao Q, Fu LJ, Li C, Wu YP, Wu HQ (2006) *Electrochem Commun* 8:1553 doi:10.1016/j.elecom.2006.07.014
17. Chung SY, Bloking JT, Chiang YM (2002) *Nat Mater* 1:123 doi:10.1038/nmat732
18. Liu H, Li C, Cao Q, Wu YP, Holze R, Wu HQ (2008) *J Solid State Electrochem* 12:1017 doi:10.1007/s10008-007-0480-4
19. Liu H, Zhang P, Li GC, Wu Q, Wu YP (2008) *J Solid State Electrochem* 12:1011 doi:10.1007/s10008-007-0478-y
20. Wang GJ, Gao J, Fu LJ, Zhao NH, Wu YP, Takamura T (2007) *J Power Sources* 174:1109 doi:10.1016/j.jpowsour.2007.06.107
21. Kim HS, Kong MZ, Kim K, Kim IJ, Gu HB (2007) *J Power Sources* 171:917 doi:10.1016/j.jpowsour.2007.06.028
22. Fu LJ, Zhang HP, Cao Q, Wang GJ, Yang LC, Wu YP (2009) *Microporous Mesoporous Mater* 117:515 doi:10.1016/j.micro.2008.07.008